Ground state of dipolar hard spheres confined in channels

Florian Deißenbeck
Institut für Theoretische Physik II, Weiche Materie: Heinrich-Heine-Universität Düsseldorf, Universitätsstr. 1, 40225 Düsseldorf, Germany

Hartmut Löwen
Institut für Theoretische Physik II, Weiche Materie: Heinrich-Heine-Universität Düsseldorf, Universitätsstr. 1, 40225 Düsseldorf, Germany

Erdal C. Oğuz
School of Mechanical Engineering and The Sackler Center for Computational Molecular and Materials Science, Tel Aviv University, Tel Aviv 6997801, Israel

(Received 27 March 2018; published 14 May 2018)

We investigate the ground state of a classical two-dimensional system of hard-sphere dipoles confined between two hard walls. Using lattice sum minimization techniques we reveal that at fixed wall separations, a first-order transition from a vacuum to a straight one-dimensional chain of dipoles occurs upon increasing the density. Further increase in the density yields the stability of an undulated chain as well as nontrivial buckling structures. We explore the close-packed configurations of dipoles in detail, and we find that, in general, the densest packings of dipoles possess complex magnetizations along the principal axis of the slit. Our predictions serve as a guideline for experiments with granular dipolar and magnetic colloidal suspensions confined in slitlike channel geometry.

DOI: 10.1103/PhysRevE.97.052608

I. INTRODUCTION

The anisotropy of the dipole-dipole interaction causes an ensemble of magnetic balls to self-assemble into nontrivial ground states at zero temperature [1–6]. For example, N hard spheres with a central dipole-dipole interaction exhibit ground-state clusters which cross over from linear chains to rings and to tubes as N grows [7,8], whereas similar clusters have also been observed for anisotropically shaped magnetic particles at finite temperatures [9,10]. Other ground-state structures have been explored for spheres with shifted dipole moments [11–14], for spheres in an external magnetic field [15], and confined onto the plane [16,17]. Magnetic hard spheres are realized in the macroworld as heavy balls [18] and granulates [19], yet a plethora of possibilities are found in the mesoscopic regime of magnetic colloids [20–31], magnetic nanoparticles [32–34] (in particular, when the magnetic interaction energy dominates thermal fluctuations), colloidal particles with an induced electric dipole moment [35,36], and dipolar dusty plasmas [37]. As these particles and their clusters constitute the main building blocks of prospective materials such as ferromagnetic filaments [38–40] for the creation of microdevices and for magnetorheological fluids and ferrogels with tunable and unusual viscoelastic properties [41–44], an understanding of their structure is of prime interest.

In this work, we explore the ground state of classical hard-sphere dipoles in two dimensions which are confined between two narrow walls in a slit geometry (a "channel"). If the slit width coincides exactly with the hard-sphere diameter, there is only a one-dimensional degree of translational freedom for the sphere centers. In this special limit, a vacuum coexists with a closely packed linear chain of touching dipoles with head-to-tail attractive configuration. Here, we study the nontrivial effect of a wider slit where geometric packing effects of the disks tends to widen the chain by buckling [45] but the dipolar interaction still keeps the particle chain aligned. As a result of this competition, we find that various *undulated chains* are the minimal potential-energy structure at densities slightly higher than for the straight chain. The "spin structure" of the magnetic moments is nontrivial though mainly aligned with the slit. The opposite limit of high density is dictated by the close-packing problem of disks between two hard lines. We revisit this elementary geometric problem and analyze the spin structure in close-packed configurations, which, in general, possess nontrivial complex magnetizations. In principle, our predictions are verifiable in experiments with granular dipolar particles and confined magnetic colloidal suspensions and they display relevance for the flow of magnetorheological suspensions through microfluidic devices.

II. MODEL

In our model, we consider N dipolar hard spheres of diameter σ that are confined in a slitlike geometry between two parallel hard walls. We restrict ourselves to the situation where all particles lie in the (x,y) plane. This restriction yields their magnetic moments to be coplanar with the same plane in the ground state [21], and as such, our system can be portrayed as an effective two-dimensional system of magnetic hard disks confined between two hard lines of length L and separation H (see Fig. 1). For convenience, this separation direction is taken along the y direction. The potential of interaction $U(\vec{r}_{ij})$ between two constitutive particles i and j whose centers are located at $\vec{r}_i$ and $\vec{r}_j$ reads as

$$U(\vec{r}_{ij}) = \frac{\mu_0}{4\pi}\left[\frac{\vec{m}_i\cdot\vec{m}_j}{r_{ij}^3} - 3\frac{(\vec{m}_i\cdot\vec{r}_{ij})(\vec{m}_j\cdot\vec{r}_{ij})}{r_{ij}^5}\right] \quad (1)$$

 ©2018 American Physical Society

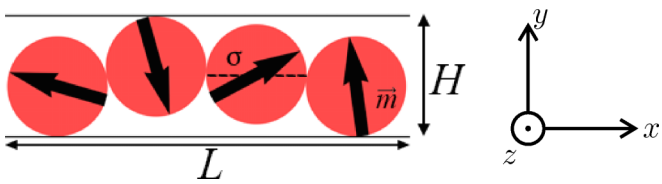

FIG. 1. Schematic illustration of dipolar hard spheres of diameter σ confined between two hard walls of separation H and length L. The spheres possess magnetic moments $\vec{m}$ and are further confined onto the (x,y) plane.

for $r_{ij} \geqslant \sigma$ or infinite otherwise, where μ_0 represents the vacuum permeability, and $r_{ij} = |\vec{r}_{ij}| = |\vec{r}_j - \vec{r}_i|$ is the interparticle distance between the spheres possessing the dipole moments $\vec{m}_i$ and $\vec{m}_j$ of equal magnitude m. At zero temperature, for a given reduced line density $\eta = N\sigma/L$, the system will minimize its potential energy per particle and the resulting structure will solely depend on the reduced slit width H/σ.

We employ three different approaches to study the phase behavior of our system in its entireness: (i) we theoretically determine the stability regime of undulated chains upon slight increase of the density beyond $\eta_{\rm ch} = 1$ at which the linear magnetic chain is stable, (ii) we perform a numerical penalty optimization method to efficiently find close-packed structures at relatively high densities $\eta_{\rm cp}$, and (iii) we carry out lattice sum minimizations to obtain the ground-state structures at densities interpolating between $\eta_{\rm ch}$ and $\eta_{\rm cp}$. The details of each method are provided in the following paragraphs.

We wish to describe first our lattice-sum technique. At each prescribed reduced density η and reduced slit width H/σ, we perform lattice sum minimizations for a broad set of candidate structures, which we take to be two-dimensional crystals with periodicity along the x direction, and confined along the y direction by the slit (cf. Fig. 1). We consider structures with a rectangular primitive cell containing up to $n = 6$ particles. Without any further restriction, we minimize the energy per particle with respect to the particle coordinates in the cell and the alignments of the two-dimensional dipole moments.

III. RESULTS

The resulting ground-state phase diagram in the $(\eta, H/\sigma)$ plane is demonstrated in Fig. 2(a) for $0 \leqslant \eta \lesssim 1.05$ and $1 \leqslant H/\sigma \leqslant 1.3$. The phase diagram exhibits a relatively large coexistence regime between the vacuum at $\eta = 0$ [purple line in Fig. 2(a)] and the linear chain of touching particles with head-to-tail attractive dipole configurations at the density $\eta_{\rm ch} = 1$ [blue line in Fig. 2(a)]. The linear chain $1C$ is schematically depicted in Fig. 2(b). Upon increasing the density beyond $\eta_{\rm ch}$, we observe the stability of undulated chains within the purple area shown in Fig. 2(a). The undulations of the magnetic chain are caused by an interplay of the geometry that favors a buckled chain for slit widths $H/\sigma > 1$ and densities $\eta > \eta_{\rm ch}$ due to an efficient packing and the attractive head-to-tail alignment of the dipoles favoring the straight chain. To investigate the stability of the undulated chain, we have calculated its total potential energy by taking into account its bending energy. Since lattice-sum minimization techniques are inappropriate to determine the energy of highly complex undulated phase structures with a large number of particles per unit cell that even diverge as $\eta \to \eta_{\rm ch}$ for $\eta > \eta_{\rm ch}$, we have used a different approach to detect such stable undulations as will be described in the following.

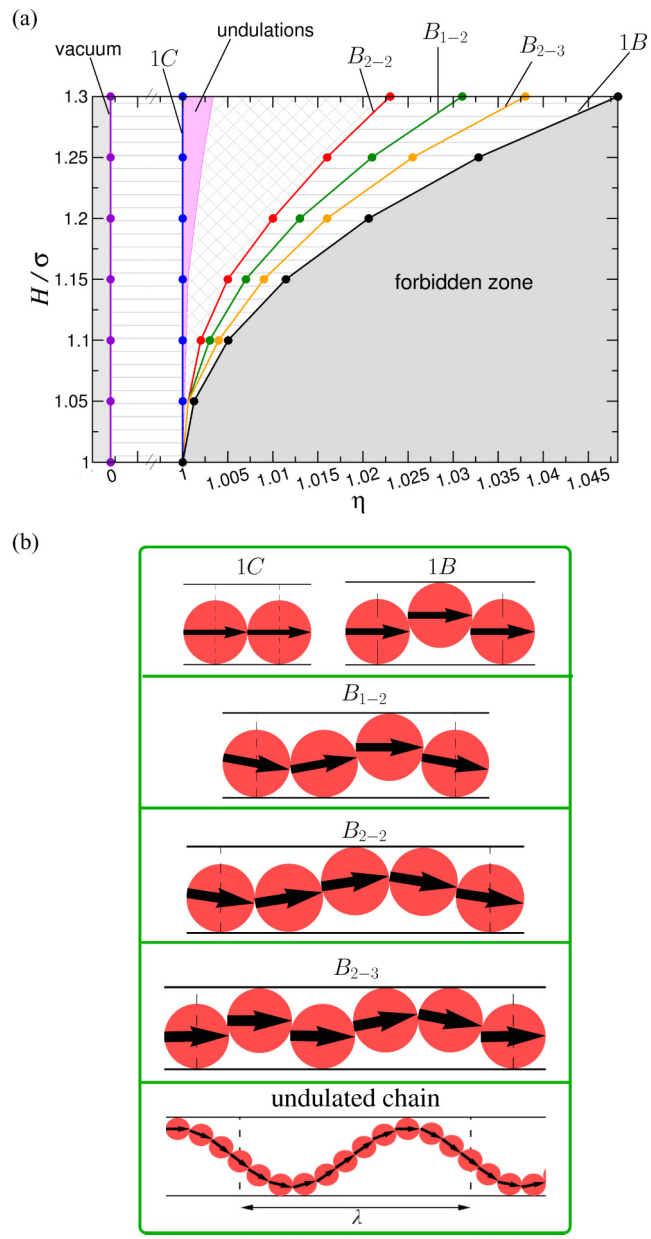

FIG. 2. (a) Ground-state phase diagram of confined dipolar hard spheres as a function of the reduced slit width H/σ and the reduced density η. The straight chain $1C$ (blue line) coexists with vacuum (purple line, $\eta = 0$) at densities $\eta < 1$, whereas for $\eta > 1$ undulated chain (purple area), the nontrivial buckling phases B_{2-2} (red curve), B_{1-2} (green curve), and B_{2-3} (yellow curve) as well as the zigzag phase $1B$ (black curve) become stable. The gray area indicates the forbidden zone beyond the densest packing regime. The dashed areas correspond to the coexistence regimes between two neighboring phases, whereas the hatched area may accommodate further phases that have not been investigated in this work. (b) Schematics of the stable phase structures shown in (a). The vertical dashed lines mark the corresponding unit cells, and λ in the most lower schematic indicates the wavelength of the undulated chain with a sinusoidal form.

We model the undulated chain as a continuous object uniformly carrying dipolar hard spheres. We assume that the linear chain undulates into periodic sinusoidal structures with a density-dependent wavelength λ as schematically illustrated in Fig. 2(b). Thus, we parametrize the contour line of the wave that passes through the particle centers by $f(x) = \frac{H-\sigma}{2}\cos(kx)$, with $k = 2\pi/\lambda$. The wavelength λ relates to the density via $\eta = l_c/\lambda$, where $l_c = \int_0^\lambda \sqrt{1 + f'(x)^2}dx$ denotes the contour length of the corresponding wave. Inserting $f(x)$ into l_c yields the equality $2\pi\eta - E[2\pi, -k(H-\sigma)/2] = 0$, from which we obtain k (and thus λ) for a given reduced density η. Here, E stands for the incomplete elliptic integral of the second kind.

Having established the exact form of the undulation wave with the corresponding wavelength, we will now determine its potential energy per particle, u_{und}, given as

$$u_{\text{und}} = u_{\text{ch}} + \frac{\gamma}{N}\int_0^{l_c} \frac{1}{R(s)^2}ds. \tag{2}$$

The first term on the right-hand side, u_{ch}, describes the magnetic energy per particle in the straight chain as dictated by the pair interaction potential of Eq. (1), and the second term the elastic bending energy per particle, respectively. $R(s)$ denotes the curvature radius of the wave as a function of its arc length $s(x) = \int_0^x \sqrt{1 + f'(x')^2}dx'$, whereas γ stands for the bending rigidity of the magnetic chain as will be determined in the following.

To obtain the bending rigidity γ, we follow the approach proposed in Ref. [7]; namely, we calculate γ by identifying the bending energy with the energy difference of a closed ring of radius R carrying N touching particles and a straight infinite chain. We consider the magnetic moments in the ring configuration to be oriented tangentially on the bending circle. The tangential alignment has been theoretically shown to minimize the ring's potential energy per particle u_{ring} in [46], and it has been demonstrated experimentally with cobalt nanoparticles in small systems in [33]. Using the relation $u_{\text{ring}}(R) - u_{\text{ch}} \sim \gamma/R^2 + O(R^{-4})$, and ignoring the higher order terms in R, the bending rigidity γ is given as

$$\gamma = \lim_{R\to\infty}[u_{\text{ring}}(R) - u_{\text{ch}}]R^2. \tag{3}$$

Taking into account the closed-form expressions for the energies u_{ring} and u_{ch} (cf. [7,8,21]), we finally obtain $\gamma 4\pi\sigma^2/\mu_0 m^2 = [\zeta(3) + 1/6]/4 \approx 0.342$, where $\zeta(m) = \sum_{i=1}^{\infty} i^{-m}$ denotes the Riemann zeta function.

We calculate the total energy per particle of the undulated chain as given in Eq. (2), and compare it to the energies obtained by our lattice-sum minimizations. It is noteworthy that, as we use a continuous modeling of the undulated chain, we are able to obtain its total energy by solely determining its elastic bending energy without any numerical minimization of a particular dipolar hard-sphere configuration on an undulated chain. Clearly this continuum description of the undulated phases is only valid for wavelengths much larger than the particle diameter such that discreteness effects become negligible. As a result, we reveal the stability of the undulated chain for slightly larger densities above $\eta_{\text{ch}} = 1$ and for all slit widths. In the limit $\eta \to \eta_{\text{ch}}$ with $\eta > \eta_{\text{ch}}$, the wavelength of undulations diverge. As the reduced density increases, undulations become stable with continuously decreasing wavelengths. For instance, at $H/\sigma = 1.3$ the smallest wavelength we obtain is $\lambda \approx 16\sigma$.

The phase space between the undulated chain and the zigzag phase $1B$ at the close-packing density η_{cp} [black curve in Fig. 2(a)] displays a plethora of nontrivial buckling structures as obtained by lattice-sum minimizations. We refer to these phases as B_{2-2} ($n = 4$), B_{1-2} ($n = 3$), and B_{2-3} ($n = 5$) and we show their stability regime by the red, green, and yellow curves in Fig. 2(a), respectively. The subindices indicate the number of particles per unit cell that are distributed—-not necessarily evenly—on the two walls while being in contact with them. For instance, B_{2-3} possesses five primitive-cell particles, where two of them are in contact with the one, and three with the other wall.

For the sake of completeness, we have further investigated the phase coexistence in our system by implementing the common tangent (Maxwell) construction: The dashed areas between two neighboring phases in Fig. 2(a) demonstrate their coexistence regime. As a result, we obtain the pure one-phase stability of the nontrivial buckling phases at a single density for a given slit width, and as such, they emerge as stability lines in the $(\eta, H/\sigma)$ plane.

Attention must be paid when interpreting the hatched area in Fig. 2(a). On the one hand, it might indicate a coexistence between the undulated phases and B_{2-2}; on the other hand, further complex phases that have not been investigated in this work may occur within this area: So far, we have considered a single mode of undulation of the linear magnetic chain, namely, periodic sinusoidal wave functions. In principle, other types of undulations might take place which, if stable, are expected to appear within this hatched area. Moreover, phase structures with more than six unit-cell particles cannot be ultimately excluded. This being said, however, we do not expect any radical morphology changes of the phase diagram.

The close-packing density η_{cp} shown by the black curve in Fig. 2(a) is an upper bound of the phase space. The gray area beyond this density displays the geometrically inaccessible ("forbidden") density zone. In order to reveal the minimum-energy state of hard dipolar disks along this density, we first use the *penalty* method to find the maximum-packing configuration of hard disks. This method as implemented in [47,48] describes an efficient algorithm to circumvent the discontinuous and constrained optimization of the free space under the constraint of nonoverlapping particles. By adding a penalty term that depends continuously on the overlap area of two disks, we obtain a continuous and unconstrained penalty function which can be minimized in the classic way to predict the optimal particle coordinates. Subsequently, in a given densest packing structure, we first assign magnetic moments to each disk and we then minimize the potential energy with respect to the alignments of those moments by our lattice sum minimization technique. As a result, we unveil the zigzag structure $1B$ with $n = 2$, where the dipole moments are all aligned parallel to the x axis [cf. the corresponding schematic in Fig. 2(b)].

Next, we wish to examine in detail the magnetic spin structure, i.e., the orientations of the magnetic moments, of close-packed hard disks for larger slit widths. To this end, we first extend our geometrical study of the densest packings up

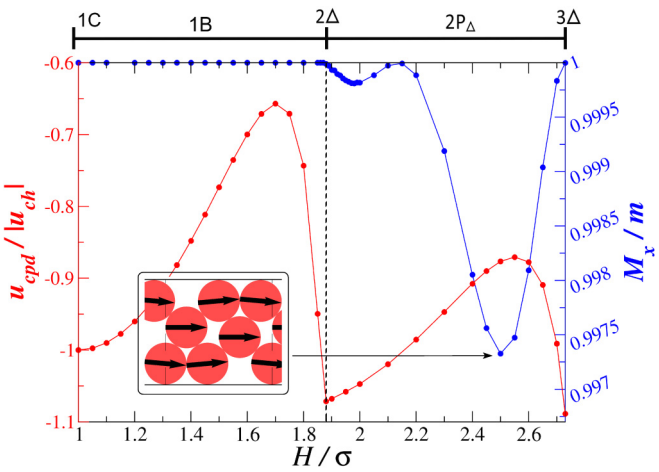

FIG. 3. Potential energy per particle of closed-packed dipolar hard spheres (left axis) and their total magnetization per particle in the parallel direction to the walls (right axis). The corresponding close-packed structures are shown in the upper panel. The inset provides a schematic illustration of dipolar $2P_\triangle$ at $H/\sigma = 2.5$.

to $H/\sigma \leqslant \sqrt{3}+1$. In particular, we investigate the regime between the linear chain $1C$ at $H/\sigma = 1$ and the triangular trilayer $3\triangle$ at $H/\sigma = \sqrt{3}+1$. We obtain the fundamental sequence $w\triangle \to (w+1)\triangle$ as well as the intermediate phases $1B$ and $2P_\triangle$ as reported in [49,50], where $w \geqslant 2$ denotes the number of parallelly stacked and staggered chains aligned with the walls, corresponding to slices of the regular triangular lattice. The phases $w\triangle$ are only best packed at discrete values of the slit width, $H_w/\sigma = (w-1)\sqrt{3}/2 + 1$, where the layers exactly fit between the walls. The resulting cascade of close-packed structures reads as $1C \to 1B \to 2\triangle \to 2P_\triangle \to 3\triangle$, and it is shown in the upper panel of Fig. 3.

Having elucidated the close-packed structures of confined hard disks, we identify their energy-minimizing spin configurations using our lattice-sum method. The resulting potential energy per particle u_{cpd} of close-packed dipolar hard spheres is shown in Fig. 3. We further calculate the total magnetization per particle along the x direction by

$$M_x = \frac{1}{n}\sum_{i=1}^{n} m \cos\theta_i, \tag{4}$$

where θ_i denotes the angle between the magnetic moment $\vec{m}_i$ and the x axis. In Fig. 3, M_x is plotted for different densest packings as a function of H/σ. We observe that the phases $2\triangle$ and $3\triangle$ as well as the zigzag phase $1B$ exhibit $M_x = m$ as their moments are all aligned parallel to the x axis. The phase $2P_\triangle$ possesses, however, a nontrivial structure of the magnetic moments that are rotated with respect to the x axis as shown in the inset of Fig. 3 for $H/\sigma = 2.5$. Consequently, the total magnetization M_x differs slightly from the magnetization m of a straight chain.

IV. CONCLUSIONS

In conclusion we have explored the ground-state structures of strongly confined magnetic disks in a slit geometry and have predicted a novel structure of undulated chains which emerge as a compromise between packing efficiency and magnetic dipole moment alignment. This simple model system could be realized either in the granular or in the colloidal context. For colloids, the two dimensionality of our model is a standard setup, and the slit geometry can be imposed by microchannels (see, e.g., [51]) or by strong external fields. Another promising direction is the structure formation of colloids under adaptive confinement where the corresponding boundaries are made of a subset of constitutive particles fixed with optical tweezers [52,53]. Furthermore, for the future, an ensemble of active or swimming magnetic particles in a slit would be a fascinating topic where the emerging clusters are not static but dynamic [54,55]. Moreover, more general models including an external magnetic field [56] or harmonic confining potential and an out-of-plane orientation of the dipole moments can be explored using similar techniques as presented here. Finally, the fact that magnetization can be tuned paves the way for microdevices to control the magnetization intrinsically by design architecture.

ACKNOWLEDGMENTS

We thank Frank Smallenburg for fruitful discussions. Financial support by the German Research Foundation (DFG) within project LO 418/19-1 is acknowledged.

[1] R. Tao and J. M. Sun, Ground state of electrorheological fluids from Monte Carlo simulations, Phys. Rev. A **44**, R6181 (1991).
[2] B. Groh and S. Dietrich, Crystal structures and freezing of dipolar fluids, Phys. Rev. E **63**, 021203 (2001).
[3] A. P. Hynninen and M. Dijkstra, Phase Diagram of Dipolar Hard and Soft Spheres: Manipulation of Colloidal Crystal Structures by an External Field, Phys. Rev. Lett. **94**, 138303 (2005).
[4] D. Levesque and J.-J. Weis, Stability of solid phases in the dipolar hard sphere system, Mol. Phys. **109**, 2747 (2012).
[5] L. Spiteri and R. Messina, Dipolar Crystals: The Crucial Role of the Clinohexagonal Prism Phase, Phys. Rev. Lett. **119**, 155501 (2017).
[6] D. Levesque, New solid phase of dipolar systems, Condens. Matter Phys. **20**, 33601 (2017).
[7] D. Vella, E. du Pontavice, C. L. Hall, and A. Goriely, The magneto-elastica: from self-buckling to self-assembly, Proc. R. Soc. A **470**, 20130609 (2013).
[8] R. Messina, L. A. Khalil, and I. Stanković, Self-assembly of magnetic balls: From chains to tubes, Phys. Rev. E **89**, 011202(R) (2014).
[9] P. Tierno, Recent advances in anisotropic magnetic colloids: Realization, assembly and applications, Phys. Chem. Chem. Phys. **16**, 23515 (2014).
[10] F. Martinez-Pedrero, A. Cebers, and P. Tierno, Orientational dynamics of colloidal ribbons self-assembled from microscopic magnetic ellipsoids, Soft Matter **12**, 3688 (2016).
[11] S. S. Kantorovich, R. Weeber, J. J. Cerda, and C. Holm, Ferrofluids with shifted dipoles: Ground state structures, Soft Matter **7**, 5217 (2011).

[12] M. Klinkigt, R. Weeber, S. S. Kantorovich, and C. Holm, Cluster formation in systems of shifted-dipole particles, Soft Matter **9**, 3535 (2013).
[13] E. V. Novak, E. S. Pyanzina, and S. S. Kantorovich, Behaviour of magnetic Janus-like colloids, J. Phys.: Condens. Matter **27**, 234102 (2015).
[14] A. B. Yener and S. H. L. Klapp, Self-assembly of three-dimensional ensembles of magnetic particles with laterally shifted dipoles, Soft Matter **12**, 2066 (2016).
[15] R. Messina and I. Stanković, Assembly of magnetic spheres in strong homogeneous magnetic field, Physica A **466**, 10 (2017).
[16] T. A. Prokopieva, V. A. Danilov, S. S. Kantorovich, and C. Holm, Ground state structures in ferrofluid monolayers, Phys. Rev. E **80**, 031404 (2009).
[17] M. A. Annunziata, A. M. Menzel, and H. Löwen, Hardening transition in a one-dimensional model for ferrogels, J. Chem. Phys. **138**, 204906 (2013).
[18] J. Schönke, T. M. Schneider, and I. Rehberg, Infinite geometric frustration in a cubic dipole cluster, Phys. Rev. B **91**, 020410(R) (2015).
[19] N. Vandewalle and S. Dorbolo, Magnetic ghosts and monopoles, New J. Phys. **16**, 013050 (2014).
[20] K. Zahn and G. Maret, Dynamic Criteria for Melting in Two Dimensions, Phys. Rev. Lett. **85**, 3656 (2000).
[21] R. Messina and I. Stanković, Self-assembly of magnetic spheres in two dimensions: The relevance of onion-like structures, Eur. Phys. Lett. **110**, 46003 (2015).
[22] L. Baraban, D. Makarov, M. Albrecht, N. Rivier, P. Leiderer, and A. Erbe, Frustration-induced magic number clusters of colloidal magnetic particles, Phys. Rev. E **77**, 031407 (2008).
[23] W. Wen, L. Zhang, and P. Sheng, Planar Magnetic Colloidal Crystals, Phys. Rev. Lett. **85**, 5464 (2000).
[24] R. M. Erb, H. S. Son, B. Samanta, V. M. Rotello, and B. B. Yellen, Magnetic assembly of colloidal superstructures with multipole symmetry, Nature (London) **457**, 999 (2009).
[25] R. Alert, P. Tierno, and J. Casademunt, Mixed-order phase transition in a colloidal crystal, Proc. Natl. Acad. Sci. USA **114**, 12906 (2017).
[26] A. I. Abrikosov, S. Sacanna, A. P. Philipse, and P. Linse, Self-assembly of spherical colloidal particles with off-centered magnetic dipoles, Soft Matter **9**, 8904 (2013).
[27] M. Klokkenburg, R. P. A. Dullens, W. K. Kegel, B. H. Erné, and A. P. Philipse, Quantitative Real-Space Analysis of Self-Assembled Structures of Magnetic Dipolar Colloids, Phys. Rev. Lett. **96**, 037203 (2006).
[28] G. Steinbach, S. Gemming, and A. Erbe, Non-equilibrium dynamics of magnetically anisotropic particles under oscillating fields, Eur. Phys. J. E **39**, 69 (2016).
[29] S. G. Jones, N. Abbasi, B.-U. Moona, and S. S. H. Tsai, Microfluidic magnetic self-assembly at liquid-liquid interfaces, Soft Matter **10**, 2016 (2016).
[30] A. Darras, J. Fiscina, M. Pakpour, N. Vandewalle, and G. Lumay, Ribbons of superparamagnetic colloids in magnetic field, Eur. Phys. J. E **39**, 47 (2016).
[31] J. Yan, K. Chaudhary, S. C. Bae, J. A. Lewis, and S. Granick, Colloidal ribbons and rings from Janus magnetic rods, Nat. Commun. **4**, 1516 (2013).
[32] S. M. Taheri, M. Michaelis, T. Friedrich, B. Förster, M. Drechsler, F. M. Römer, P. Bösecke, T. Narayanane, B. Weber, I. Rehberg, S. Rosenfeldt, and S. Förster, Self-assembly of smallest magnetic particles, Proc. Natl. Acad. Sci. USA **112**, 14484 (2015).
[33] S. L. Tripp, R. E. Dunin-Borkowski, and A. Wei, Flux closure in self-assembled cobalt nanoparticle rings, Angew. Chem., Int. Ed. **42**, 5591 (2003).
[34] D. V. Talapin, E. V. Shevchenko, C. B. Murray, A. V. Titov, and P. Král, Dipole-dipole interactions in nanoparticle superlattices, Nano Lett. **7**, 1213 (2007).
[35] A. Yethiraj and A. van Blaaderen, A colloidal model system with an interaction tunable from hard sphere to soft and dipolar, Nature (London) **421**, 513 (2003).
[36] K. Kang and J. K. G. Dhont, Double-layer polarization induced transitions in suspensions of colloidal rods, Europhys. Lett. **84**, 14005 (2008).
[37] P. C. Brandt, A. V. Ivlev, and G. E. Morfill, Solid phases in electro- and magnetorheological systems, J. Chem. Phys. **130**, 204513 (2009).
[38] R. Messina and L. Spiteri, On the interaction of dipolar filaments, Eur. Phys. J. E **39**, 81 (2016).
[39] L. Goyeau, R. Livanovics, and A. Cēbers, Dynamics of a flexible ferromagnetic filament in a rotating magnetic field, Phys. Rev. E **96**, 062612 (2017).
[40] H.-H. Boltz and S. Klumpp, Buckling of elastic filaments by discrete magnetic moments, Eur. Phys. J. E **40**, 86 (2017).
[41] S. Odenbach, Ferrofluids, J. Phys.: Condens. Matter **18** (2006).
[42] P. Cremer, H. Löwen, and A. M. Menzel, Tailoring superelasticity of soft magnetic materials, Appl. Phys. Lett. **107**, 171903 (2015).
[43] S. Huang, G. Pessot, P. Cremer, R. Weeber, C. Holm, J. Nowak, S. Odenbach, A. M. Menzel, and G. K. Auernhammer, Buckling of paramagnetic chains in soft gels, Soft Matter **12**, 228 (2016).
[44] A. Mughal, L. Laurson, G. Durin, and S. Zapperi, Effect of dipolar interactions for domain-wall dynamics in magnetic thin films, IEEE Trans. Magn. **46**, 228 (2010).
[45] M. Schmidt and H. Löwen, Phase diagram of hard spheres confined between two parallel plates, Phys. Rev. E **55**, 7228 (1997).
[46] B. Kiani, D. Faivre, and S. Klumpp, Elastic properties of magnetosome chains, New J. Phys. **17** 043007 (2015).
[47] E. C. Oğuz, M. Marechal, F. Ramiro-Manzano, I. Rodriguez, R. Messina, F. J. Meseguer, and H. Löwen, Packing Confined Hard Spheres Denser with Adaptive Prism Phases, Phys. Rev. Lett. **109**, 218301 (2012).
[48] L. Assoud and R. Messina, Penalty method to predict crystal structures involving hard-core interactions, Phys. Rev. E **83**, 036113 (2011).
[49] J. Molnár, Packing of congruent spheres in a strip, Acta Math. Hung. **31**, 173 (1978).
[50] Z. Füredi, The densest packing of equal circles into a parallel strip, Discrete Comput. Geom. **6**, 95 (1991).
[51] M. Koppl, P. Henseler, A. Erbe, P. Nielaba, and P. Leiderer, Layer Reduction in Driven 2D-Colloidal Systems through Microchannels, Phys. Rev. Lett. **97**, 208302 (2006).
[52] I. Williams, E. C. Oğuz, T. Speck, P. Bartlett, H. Löwen, and C. P. Royall, Transmission of torque at the nanoscale, Nat. Phys. **12**, 98 (2016).

[53] I. Williams, E. C. Oğuz, R. L. Jack, P. Bartlett, H. Löwen, and C. P. Royall, The effect of boundary adaptivity on hexagonal ordering and bistability in circularly confined quasi hard discs, J. Chem. Phys. **140**, 104907 (2014).

[54] A. Kaiser, K. Popowa, and H. Löwen, Active dipole clusters: From helical motion to fission, Phys. Rev. E **92**, 012301 (2015).

[55] F. Guzman-Lastra, A. Kaiser, and H. Löwen, Fission and fusion scenarios for magnetic microswimmer clusters, Nat. Commun. **7**, 13519 (2016).

[56] D. Morphew and D. Chakrabarti, Hierarchical self-assembly of colloidal magnetic particles into reconfigurable spherical structures, Nanoscale **7**, 8343 (2015).